DO-TH 04/09

Testing the Equivalent Photon Approximation of the Proton in the Process $ep \to \nu W X$

Cristian Pisano*

Institut für Physik, Universität Dortmund, D 44221 Dortmund, Germany

(Dated: February 2, 2008)

Abstract

The accuracy of the equivalent photon approximation (EPA) of the proton in describing the inelastic process $ep \to \nu W X$ is investigated. In particular, the scale dependence of the corresponding inelastic photon distribution is discussed. Furthermore, an estimate of the total number of events, including the ones coming from the elastic and quasi-elastic channels of the reaction, is given for the HERA collider.

*Electronic address: pisano@harpo.physik.uni-dortmund.de

I. INTRODUCTION

The equivalent photon approximation (EPA) of the nucleon N ($= p$, n) is a technical device which allows for a simpler and more efficient calculation of any photon-induced subprocess, whose cross section can be written as a convolution of the probability that the nucleon radiates off a photon (equivalent photon distribution) with the corresponding real photoproduction cross section. The polarized and unpolarized photon distributions of the nucleon, evaluated in the EPA, have been computed theoretically [1] and the possibility of their experimental determination has also been demonstrated [2, 3, 4, 5]. Both of them consist of two components, an elastic one, due to $N \to \gamma N$, and an inelastic one, due to $N \to \gamma X$, with $X \neq N$. The reliability of the EPA remains, however, to be studied.

In [6] the unpolarized elastic photon distribution was tested in the case of νW production in the process $ep \to \nu W p$. The relative error of the cross section as calculated in the EPA with respect to the exact result was shown as a function of $\sqrt{S}$, in the range $100 \leq \sqrt{S} \leq 1800$ GeV. The agreement turned out to be very good, the approximation reproducing the exact cross section within less than one percent. Motivated by this results, our aim here is to check if the same holds in the inelastic channel.

The process $ep \to \nu W X$ has been widely studied by several authors [7, 8, 9, 10, 11]. Its relevance is related to the possibility of measuring the three-vector-boson coupling $WW\gamma$, which is a manifestation of the nonabelian gauge symmetry upon which the Standard Model is based. The observation of the vector boson self interaction would be a crucial test of the theory. Furthermore, such a reaction is also an important background to a number of processes indicating the presence of new physics. The lightest Supersymmetric Standard Model particle has no charge and interacts very weakly with matter; it means that, exactly as the neutrino from the Standard Model, it escapes the detector unobserved and can be recognized only by missing momentum. This implies that a detailed study of the processes with neutrinos in the final states is necessary to distinguish between the new physics of the Supersymmetric Standard Model and the physics of the Standard Model. At the HERA collider energies ($\sqrt{S} = 318$ GeV) the $ep \to \nu W X$ cross section is much smaller than the one for $ep \to eWX$ [8, 9], also sensitive to the $WW\gamma$ coupling, due to the presence in the latter of an additional Feynman graph where an almost real photon and a massless quark are exchanged in a u-channel configuration (u-channel pole). The dominance of the

process $ep \to eWX$ justifies the higher theoretical and experimental [12] attention that it has received so far, as compared to $ep \to \nu WX$. One way of limiting the problem of the low number of νW events at HERA would be to consider also the elastic and quasi-elastic channels of the reaction, as will be discussed in Section III.

It is worth mentioning that not all the calculations of the $ep \to \nu WX$ event rates available in the literature, in which only the photon exchange is considered (see Fig. 1), are in agreement, as already pointed out in [11]. In particular, the numerical estimate of the cross section for HERA energies presented in [7, 8], obtained in the EPA approach, is one half of the one published in [11], obtained within the framework of the helicity amplitude formalism without any approximation. The value given in [10] is even bigger than the one in [11]: all these discrepancies cannot be due to the slightly different kinematical cuts employed in the papers cited above and stimulate a further analysis. Our results agree with [7, 8].

The plan of this paper is as follows. In Section II we calculate the exact cross section for the inelastic channel in a manifestly covariant way and we show in which kinematical region it is supposed to be well described by the EPA. The formulae for the corresponding elastic cross sections, both the exact and the one evaluated in the EPA, are also given. The numerical results are discussed in Section III. The summary is given in Section IV.

II. THEORETICAL FRAMEWORK

The νW production from inelastic ep scattering,

$$e(l) + p(P) \to \nu(l') + W(k') + X(P_X), \tag{2.1}$$

is described, considering only one photon exchange, by the Feynman diagrams depicted in Fig. 1. The four-momenta of the particles are given in the brackets; $P_X = \sum_{X_i} P_{X_i}$ is the sum over all momenta of the produced hadronic system. We introduce the invariants

$$S = (P + l)^2, \qquad \hat{s} = (l + k)^2, \qquad Q^2 = -k^2, \tag{2.2}$$

where $k = P - P_X$ is the four-momentum of the virtual photon. Following [2], the integrated cross section can be written as

$$\sigma_{\rm inel}(S) \;=\; \frac{\alpha}{4\pi(S-m^2)^2} \int_{W^2_{\rm min}}^{W^2_{\rm max}} dW^2 \int_{\hat{s}_{\rm min}}^{(\sqrt{S}-W)^2} d\hat{s} \int_{Q^2_{\rm min}}^{Q^2_{\rm max}} \frac{dQ^2}{Q^4} \int_{\hat{t}_{\rm min}}^{\hat{t}_{max}} d\hat{t} \int_0^{2\pi} d\varphi^* \Big\{ \Big[\Big(2\,\frac{S-m^2}{\hat{s}+Q^2}$$

$$\times \Big(1 - \frac{S-m^2}{\hat{s}+Q^2}\Big) + (W^2-m^2)\Big(\frac{2\,(S-m^2)}{Q^2(\hat{s}+Q^2)} - \frac{1}{Q^2} + \frac{m^2-W^2}{2\,Q^4}\Big)\Big)$$
$$\times [3X_1(\hat{s},Q^2,\hat{t}) + X_2(\hat{s},Q^2,\hat{t})] + \Big(\frac{1}{Q^2}(W^2-m^2) + \frac{(W^2-m^2)^2}{2\,Q^4} + \frac{2m^2}{Q^2}\Big)$$
$$\times [X_1(\hat{s},Q^2,\hat{t}) + X_2(\hat{s},Q^2,\hat{t})] - X_1(\hat{s},Q^2,\hat{t})\Big]F_2(x_B,Q^2)\frac{x_B}{2}$$
$$- X_2(\hat{s},Q^2,\hat{t})F_1(x_B,Q^2)\Big\}, \tag{2.3}$$

where W^2 indicates the invariant mass squared of the produced hadronic system X, φ^* denotes the azimuthal angle of the outgoing $\nu - W$ system in the $\nu - W$ CM frame, and

$$x_B = \frac{Q^2}{W^2 + Q^2 - m^2} \tag{2.4}$$

is the Bjorken variable. $F_{1,2}(x_B, Q^2)$ are the structure functions of the proton and the two invariants $X_{1,2}(\hat{s}, Q^2, t)$, which contain all the information about the subprocess $e\gamma^* \to \nu W$, are given by

$$X_1(\hat{s},Q^2,\hat{t}) \;=\; \frac{\alpha G_F}{2\sqrt{2}\pi}\frac{Q^2M_W^2}{(Q^2+\hat{s})^3\,(M_W^2-\hat{t})^2}[(Q^2+\hat{s})^3 - \hat{s}(Q^2+\hat{s})^2(Q^2+\hat{s}+\hat{t})$$
$$+\;\; 2(Q^2+\hat{s})^2\hat{t} + 8(Q^2+\hat{s})\hat{t}^2 + 8\hat{t}^3] \tag{2.5}$$

and

$$X_2(\hat{s},Q^2,\hat{t}) \;=\; \frac{\alpha G_F}{2\sqrt{2}\pi}\frac{1}{\hat{s}^2(Q^2+\hat{s})(M_W^2-\hat{t})^2}\{4M_W^8(Q^2+\hat{s}) - 4M_W^6[3\hat{s}(Q^2+\hat{s})$$
$$+\;\; (2Q^2+\hat{s})\hat{t}] + 4M_W^4[\hat{s}(2\hat{s}+\hat{t})^2 + Q^2(4\hat{s}^2+2\hat{s}\hat{t}+\hat{t}^2)] - M_W^2\hat{s}$$
$$\times\;\; [Q^4\hat{s} + Q^2(9\hat{s}^2+2\hat{s}\hat{t}-4\hat{t}^2) + 4(\hat{s}+\hat{t})(2\hat{s}^2+2\hat{s}\hat{t}+\hat{t}^2)]$$
$$+\, Q^2\hat{s}^2[\hat{s}(\hat{s}+\hat{t}) +\;\; Q^2(\hat{s}+2\hat{t})]\}. \tag{2.6}$$

In Eq. (2.3) the minimum value of $\hat{s}$ is given by the squared mass of the W boson:

$$\hat{s}_{\min} = M_W^2, \tag{2.7}$$

while the limits of the integration over W^2 are:

$$W^2_{\min} = (m+m_\pi)^2, \qquad W^2_{\max} = (\sqrt{S} - \sqrt{\hat{s}_{\min}})^2, \tag{2.8}$$

where m_π is the mass of the pion. The limits $Q^2_{\min,\max}$ are given by:

$$Q^2_{\min,\max} \;=\; -m^2 - W^2 + \frac{1}{2S}\Big[(S+m^2)(S-\hat{s}+W^2)$$
$$\mp\,(S-m^2)\sqrt{(S-\hat{s}+W^2)^2 - 4SW^2}\Big], \tag{2.9}$$

and the extrema of $\hat{t}$ are

$$\hat{t}_{\max} = 0, \quad \hat{t}_{\min} = -\frac{(\hat{s}+Q^2)(\hat{s}-M_W^2)}{\hat{s}}. \tag{2.10}$$

Integrating $X_{1,2}(\hat{s}, Q^2, \hat{t})$ over φ^* and $\hat{t}$, with the limits in Eq. (2.10), one recovers Eqs. (4.1) and (4.2) of [6] respectively, times a factor of two due to a different normalization.

The EPA consists of considering the exchanged photon as real; it is possible to get the approximated cross section $\sigma_{\rm inel}^{\rm EPA}$ from the exact one, Eq. (2.3), in a straightforward way, following again [2]. We neglect m^2 compared to S and Q^2 compared to $\hat{s}$ then, from Eqs. (2.11)-(2.12),

$$X_1(\hat{s}, Q^2, \hat{t}) \approx X_1(\hat{s}, 0, \hat{t}) = 0, \tag{2.11}$$

and

$$X_2(\hat{s}, Q^2, \hat{t}) \approx X_2(\hat{s}, 0, \hat{t}) = -\frac{2\hat{s}}{\pi}\,\frac{d\hat{\sigma}(\hat{s}, \hat{t})}{d\hat{t}}, \tag{2.12}$$

where we have introduced the differential cross section for the real photoproduction process $e\gamma \to \nu W$:

$$\frac{d\hat{\sigma}(\hat{s}, \hat{t})}{d\hat{t}} = -\frac{\alpha G_F M_W^2}{\sqrt{2}\hat{s}^2}\Big(1 - \frac{1}{1+\hat{u}/\hat{s}}\Big)^2\,\frac{\hat{s}^2+\hat{u}^2+2\hat{t}M_W^2}{\hat{s}\hat{u}} \tag{2.13}$$

with $\hat{u} = (l-k')^2 = M_W^2 - \hat{s} - \hat{t}$. Eq. (2.13) agrees with the analytical result already presented in [7, 8], obtained using the helicity amplitude technique. Using Eqs. (2.11) and (2.12), we can write

$$\sigma_{\rm inel}(S) \approx \sigma_{\rm inel}^{\rm EPA} = \int_{x_{\min}}^{(1-m/\sqrt{S})^2} dx \int_{M_W^2-\hat{s}}^{0} d\hat{t}\;\gamma_{\rm inel}(x, xS)\,\frac{d\hat{\sigma}(xS, \hat{t})}{d\hat{t}}, \tag{2.14}$$

where $x = \hat{s}/S$ and $\gamma_{\rm inel}(x, xS)$ is the inelastic component of the equivalent photon distribution of the proton:

$$\begin{aligned}\gamma_{\rm inel}(x, xS) \;=\; \frac{\alpha}{2\pi}\int_x^1 dy \int_{Q^2_{\min}}^{Q^2_{\max}} \frac{dQ^2}{Q^2}\,\frac{y}{x}\Big[F_2\Big(\frac{x}{y}, Q^2\Big)\Big(\frac{1+(1-y)^2}{y^2} - \frac{2m^2x^2}{y^2Q^2}\Big) \\ - F_L\Big(\frac{x}{y}, Q^2\Big)\Big],\end{aligned} \tag{2.15}$$

with

$$Q^2_{\min} = \frac{x^2m^2}{1-x}, \qquad Q^2_{\max} = \hat{s}. \tag{2.16}$$

As pointed out in [7], there is some ambiguity in the choice of $Q^2_{\rm max}$, which is typical of all leading logarithmic approximations, and any other quantity of the same order of magnitude of $\hat{s}$, like $-\hat{t}$ or $-\hat{u}$, would be equally acceptable for $Q^2_{\rm max}$ within the limits of the EPA. The numerical effects related to the scale dependence of the inelastic photon distribution are discussed in the next section.

The cross section relative to the elastic channel, $ep \to \nu W p$, has been calculated in [6] and can be written in the form [2]

$$\begin{aligned}\sigma_{\rm el}(S) \;=\; \frac{\alpha}{8\pi(S-m^2)^2}\int_{\hat{s}_{\rm min}}^{(\sqrt{S}-m)^2} d\hat{s}\int_{t_{\rm min}}^{t_{\rm max}}\frac{dt}{t}\int_{\hat{t}_{\rm min}}^{\hat{t}_{\rm max}} d\hat{t}\int_0^{2\pi} d\varphi^*\Big\{\Big[2\,\frac{S-m^2}{\hat{s}-t}\Big(\frac{S-m^2}{\hat{s}-t}-1\Big)\\ \times\,[3X_1(\hat{s},t,\hat{t})+X_2(\hat{s},t,\hat{t})]+\frac{2m^2}{t}[X_1(\hat{s},t,\hat{t})+X_2(\hat{s},t,\hat{t})]+X_1(\hat{s},t,\hat{t})\Big]H_1(t)\\ +\,X_2(\hat{s},t,\hat{t})H_2(t)\Big\},\end{aligned} \tag{2.17}$$

with $t=-Q^2$, integrated over the range already defined by Eq. (2.9), and $\hat{s}_{\rm min}$ given by Eq. (2.7). The limits of integration of $\hat{t}$ are the same as in Eq. (2.10) and the invariants $H_{1,2}(t)$ can be expressed as

$$H_1(t)=\frac{G_E^2(t)-(t/4\,m^2)\,G_M^2(t)}{1-t/4\,m^2},\qquad H_2(t)=G_M^2(t), \tag{2.18}$$

$G_E(t)$ and $G_M(t)$ being the well-known electric and magnetic form factors of the proton, respectively. Again, in the limit $S\gg m^2$ and $\hat{s}\gg -t$, the cross section factorizes and is given by

$$\sigma_{\rm el}(S)\approx\sigma_{\rm el}^{\rm EPA}=\int_{x_{\rm min}}^{(1-m/\sqrt{S})^2} dx\int_{M_W^2-\hat{s}}^0 d\hat{t}\,\gamma_{\rm el}(x)\,\frac{d\hat{\sigma}(xS,\hat{t})}{d\hat{t}}, \tag{2.19}$$

where $x=\hat{s}/S$ and

$$\gamma_{\rm el}(x)=-\frac{\alpha}{2\pi}x\int_{t_{\rm min}}^{t_{\rm max}}\frac{dt}{t}\Big\{2\Big[\frac{1}{x}\Big(\frac{1}{x}-1\Big)+\frac{m^2}{t}\Big]H_1(t)+H_2(t)\Big\}, \tag{2.20}$$

with

$$t_{\rm min}\approx-\infty\qquad\qquad t_{\rm max}\approx-\frac{m^2x^2}{1-x}, \tag{2.21}$$

is the universal, scale independent, elastic component of the photon distribution of the proton, derived for the first time in [6].

III. NUMERICAL RESULTS

In this section, we present a numerical estimate of the cross sections for the reactions $ep \to \nu WX$ and $ep \to \nu Wp$, calculated both exactly and in the EPA, in the range $100 \leq \sqrt{S} \leq 2000$ GeV. We take $M_W = 80.42$ GeV for the mass of the W boson and $G_F = 1.1664 \times 10^{-5}$ GeV^{-2} for the Fermi coupling constant [13]. All the integrations are performed numerically. In the evaluation of Eqs. (2.3) and (2.15) we assume the LO Callan-Gross relation

$$F_L(x_B, Q^2) \;=\; F_2(x_B, Q^2) - 2x_B F_1(x_B, Q^2) \;=\; 0, \tag{3.1}$$

and we use the ALLM97 parametrization of the proton structure function $F_2(x, Q^2)$ [14], which provides a purely phenomenological, Regge model inspired, description of $F_2(x, Q^2)$, including its vanishing in the $Q^2 = 0$ limit as well as its scaling behaviour at large Q^2. The ALLM97 parametrization is supposed to hold over the entire range of x_B and Q^2 studied so far, namely $3 \times 10^{-6} < x_B < 0.85$ and $0 \leq Q^2 < 5000$ GeV^2, above the quasi-elastic region ($W^2 > 3$ GeV^2) dominated by resonances. We do not consider the resonance contribution separately but, using the so-called local duality [16], we extend the ALLM97 parametrization from the continuous ($W^2 > 3$ GeV^2) down to the resonance domain ($(m_\pi + m)^2 < W^2 < 3$ GeV^2): in this way it is possible to agree with the experimental data averaged over each resonance. In our analysis, the average value of x_B always lies within the kinematical region mentioned above, where the experimental data are available. On the contrary, the avarage value of Q^2 becomes larger than 5000 GeV^2 when $\sqrt{S} \gtrsim 1200$ GeV, so we need to extrapolate the ALLM97 parametrization beyond the region where the data have been fitted. Our conclusions do not change if we utilize a parametrization of $F_2(x_B, Q^2)$ whose behaviour at large Q^2 is constrained by the Altarelli-Parisi evolution equations, like GRV98 [15].

The electric and magnetic form factors, necessary for the determination of the elastic cross sections in Eqs. (2.17) and (2.19), are empirically parametrized as dipoles:

$$G_E(t) = \frac{1}{[1 - t/(0.71\,\text{GeV}^2)]^2}, \qquad G_M(t) = 2.79\; G_E(t). \tag{3.2}$$

At the HERA collider, where the electron and the proton beams have energy $E_e = 27.5$ GeV and $E_p = 920$ GeV respectively, the cross section is dominated by the inelastic channel: $\sigma_{\text{el}} = 2.47 \times 10^{-2}$ pb, while $\sigma_{\text{inel}} = 3.22 \times 10^{-2}$ pb; therefore the expected integrated luminosity of 200 pb^{-1} would yield a total of about 11 events/year.

Fig. 2 shows a comparison of the inelastic cross section calculated in the EPA, $\sigma_{\rm inel}^{\rm EPA}$, with the exact one, $\sigma_{\rm inel}$, as a function of $\sqrt{S}$, where several scales for $\sigma_{\rm inel}^{\rm EPA}$ are proposed, namely $Q^2_{\rm max} = \hat{s},\ -\hat{u},\ -\hat{t}$ in Eq. (2.15) . It turns out that the choice of $-\hat{t}$ does not provide an adequate description of $\sigma_{\rm inel}$, while $\hat{s}$ and $-\hat{u}$ are approximatively equivalent in reproducing $\sigma_{\rm inel}$. In particular, the choice of $-\hat{u}$ is slightly better in the range $300 \lesssim \sqrt{S} \lesssim 1000$ GeV, while $\hat{s}$ guarantees a more accurate description of the exact cross section for $\sqrt{S} \gtrsim 1000$ GeV. At HERA energies, $\sigma_{\rm inel}^{\rm EPA} = 3.64 \times 10^{-2}$ pb, 3.51×10^{-2} pb and 3.07×10^{-2} pb for $Q^2_{\rm max} = \hat{s}$, $-\hat{u}$ and $-\hat{t}$, respectively. In the following we will fix the scale to be $\hat{s}$, in analogy to our previous studies about the QED Compton scattering process in $ep \to e\gamma X$ [2, 4, 5]. In [4, 5] it was suggested that the experimental selection of only those events for which $\hat{s} > Q^2$ restricts the kinematics of the process to the region of validity of the EPA and improves the extraction the equivalent photon distribution from the exact cross section. The effect of such a cut on the reaction $ep \to \nu W X$ is shown in Fig. 3 and the reduction of the discrepancy is evident at large $\sqrt{S}$, but not at HERA energies, where $\sigma_{\rm el}$ and $\sigma_{\rm inel}$ are unchanged.

In Fig. 4 the total (elastic + inelastic) exact cross section is depicted as a function of $\sqrt{S}$, together with the approximated one. Here the kinematical constraint $\hat{s} > Q^2$ is *not* imposed on the exact cross section. The average discrepancy is reduced to be about 2%, due to the inclusion of the elastic channel, better described by the EPA (average discrepancy 0.05%). The elastic component is also shown separately, and it agrees with the curve presented in Fig. 3 of [6]. For $\sqrt{S} = 318$ GeV, $\sigma_{\rm el}^{\rm EPA} = 2.47 \times 10^{-2}$ pb, in perfect agreement with the exact value $\sigma_{\rm el}$.

We compare now our results with the ones already published. In [11], taking into account the photon exchange only (Fig. 1) and with no further approximation, fixing $M_W = 83.0$ GeV, $\sin^2\theta_W = 0.217$, $E_e = 30$ GeV, $E_p = 820$ GeV and using the parton distributions [17] (Set 1), together with the cuts $Q^2 > 4$ GeV^2 and $W^2 > 10$ GeV^2, the value $\sigma_{\rm inel} = 3.0 \times 10^{-2}$ pb was obtained. This is in contrast to $\sigma_{\rm inel} = 1.5 \times 10^{-2}$ pb, calculated using Eq. (2.3) with the same sets of cuts, values of the energies, M_W and parton distributions utilized in [11]. The authors of [11] also report the value $\sigma_{\rm inel} = 4.0 \times 10^{-2}$ pb, obtained in [10] with a similar analysis at the same energies, using $M_W = 78$ GeV and $\sin^2\theta_W = 0.217$. The lower limit on Q^2 was taken to be $O(1)$ GeV^2, but not explicitly mentioned. Even with the ALLM97 parametrization, which allows us to use no cutoff on Q^2, we get $\sigma_{\rm inel} = 3.1 \times 10^{-2}$ pb, far below 4.0×10^{-2} pb. No analytical expression of the cross section is provided in [10, 11],

which makes it difficult to understand the source of the discrepancies.

Finally, an estimate of the the $ep \to \nu W X$ cross section is also given in [7, 8], utilizing an inelastic equivalent photon distribution slightly different from the one in Eq. (2.15), which can be written in the form

$$\tilde{\gamma}_{\rm inel}(x, Q^2_{\rm max}) = \frac{\alpha}{2\pi} \int_x^1 dy\, F_2\Big(\frac{x}{y}, \langle Q^2 \rangle\Big)\ \frac{1+(1-y)^2}{x\,y}\ \log \frac{Q^2_{\rm max}}{Q^2_{\rm cut}}, \tag{3.3}$$

where

$$\langle Q^2 \rangle = \frac{Q^2_{\rm max} - Q^2_{\rm cut}}{\log \frac{Q^2_{\rm max}}{Q^2_{\rm cut}}}, \tag{3.4}$$

$Q^2_{\rm max} = x_B S - M_W^2$ and $Q^2_{\rm cut} = 1$ GeV^2. Eq. (3.3) can be obtained from Eq. (2.15) neglecting the mass term and approximating the integration over Q^2. In the calculation performed in [7, 8], $\tilde{\gamma}_{\rm inel}(x, Q^2_{\rm max})$ is convoluted with the differential cross section for the real photoproduction process in Eq. (2.13). At $\sqrt{S} = 300$ GeV, fixing $M_W = 84$ GeV, $\sin^2\theta_W = 0.217$ and using the parton distribution parametrization [17] (Set 1), we get $\sigma_{\rm inel} = 1.6 \times 10^{-2}$ pb, very close to the value 1.5×10^{-2} pb published in [7, 8].

IV. SUMMARY AND CONCLUSIONS

To summarize, we have calculated the cross section for the inelastic process $ep \to \nu W X$, both exactly and using the equivalent photon approximation (EPA) of the proton, in order to test its accuracy in the inelastic channnel and complete the study initiated in [6], limited to the elastic process $ep \to \nu W p$. The relative error of the approximated result with respect to the exact one is scale dependent; fixing the scale to be $\hat{s}$, it decreases from about 10% at HERA energies down to 0.5% for $\sqrt{S} = 1500$ GeV, then it slightly increases up to 3% for $\sqrt{S} = 2000$ GeV. In conclusion, even if not so remarkable as for the elastic channel, in which the deviation is always below one percent [6], the approximation can be considered quite satisfactory. We have compared our calculations with previous ones in the literature and found that they are in agreement with [7, 8], but disagree with [10, 11]. Furthermore, we have estimated the total number of νW events expected at the HERA collider, including the elastic and quasi-elastic channels of the reaction. The production rate turns out to be quite small, about 11 events/year, assuming a luminosity of 200 pb^{-1}, but the process could still be detected.

V. ACKNOWLEDGEMENTS

We would like to thank E. Reya and M. Glück for many helpful discussions and suggestions, as well as for a critical reading of the manuscript. Discussions with A. Mukherjee are also acknowledged. This work has been supported in part by the 'Bundesministerium für Bildung und Forschung', Berlin/Bonn.

---

[1] M. Glück, C. Pisano and E. Reya, Phys. Lett. **B 540**, 75, (2002), and references therein.

[2] A. Mukherjee and C. Pisano, Eur. Phys. J. **C 30**, 477 (2003).

[3] M. Glück, C. Pisano, E. Reya and I. Schienbein, Eur. Phys. J. **C 27**, 427 (2003).

[4] A. Mukherjee and C. Pisano, Eur. Phys. J. **C 35**, 509 (2004).

[5] A. Mukherjee and C. Pisano, Phys. Rev. **D 70** , 034029 (2004); A. Mukherjee and C. Pisano, hep-ph/0405100.

[6] B. A. Kniehl, Phys. Lett. **B 254**, 267 (1991).

[7] G. Altarelli, G. Martinelli, B. Mele and R. Rückl, Nucl. Phys. **B 262**, 204 (1985).

[8] E. Gabrielli, Mod. Phys. Lett. **A 1**, 465 (1986); Erratum ibid. **A 2**, 69 (1987).

[9] D. Atwood, U. Baur, D. Goddard, S. Godfrey and B. A. Kniehl, Proc. of 1990 Summer Study on Research Directions for the Decade, Snowmass, CO, June-July, 1990; U. Baur, J. A. M. Vermaseren and D. Zeppenfeld, Nucl. Phys. **B 375**, 3 (1992).

[10] H. Neufeld, Z. Phys. **C 17**, 145 (1983).

[11] M. Böhm and A. Rosado, Z. Phys. **C 39**, 275 (1988).

[12] H1 Collaboration, V. Andreev et al., Phys. Lett. **B 561**, 241 (2003).

[13] Particle Data Group, S. Eidelman et al., Phys. Lett. **B 592**, 1 (2004).

[14] H. Abramowicz and A. Levy, hep-ph/9712415; corrected according to a private communication by the authors.

[15] M. Glück, E. Reya and A. Vogt, Eur. Phys. J. **C 5**, 461 (1998).

[16] E. D. Bloom and F. J. Gilman, Phys. Rev. Lett. **25**, 1140 (1970); Phys. Rev. **D 4**, 2901 (1971).

[17] D. W. Duke and J. F. Owens, Phys. Rev. **D 30**, 49 (1984).

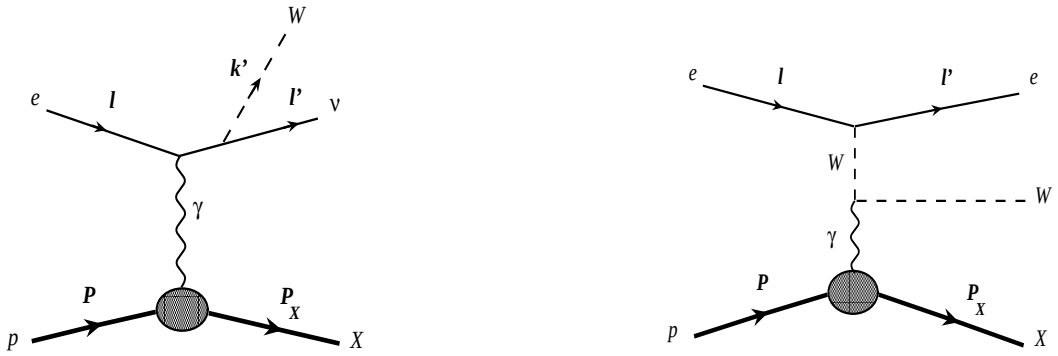

Fig. 1: Feynman diagrams for the process $ep \to \nu W X$.

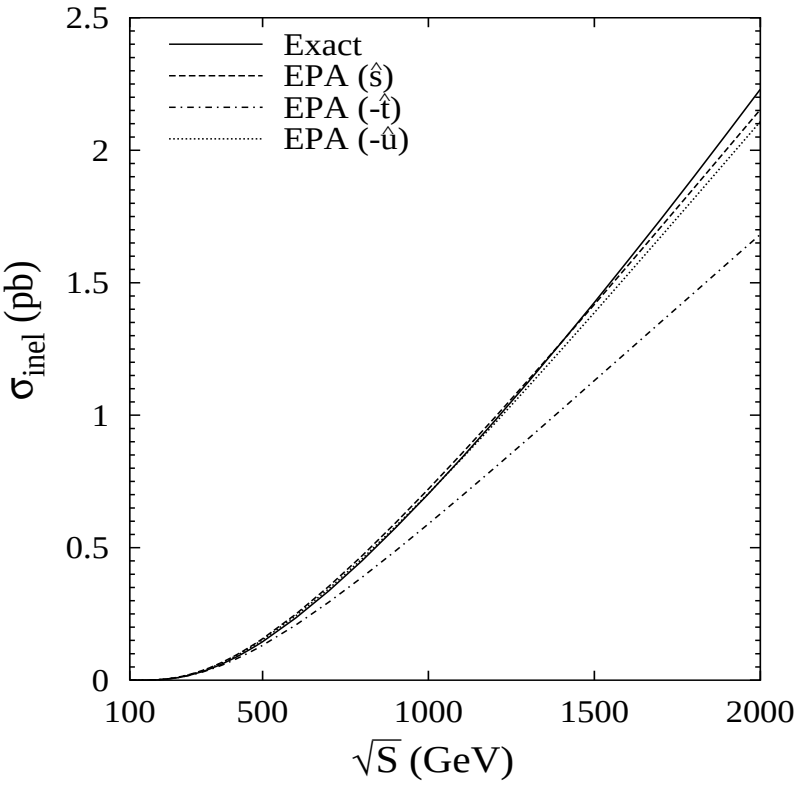

Fig. 2: Exact and approximated (EPA) inelastic cross sections of the process $ep \to \nu W X$ as functions of $\sqrt{S}$. The different scales utilized in the calculation of the approximated cross section are written in the brackets.

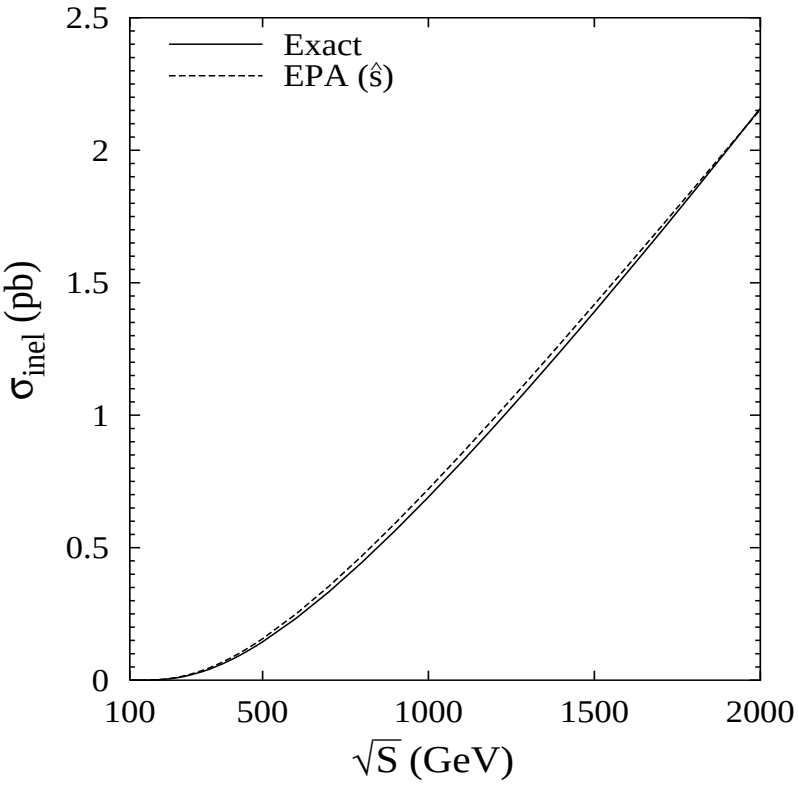

Fig. 3: Exact and approximated (EPA) inelastic cross sections of the process $ep \to \nu W X$ as functions of $\sqrt{S}$. The scale $\hat{s}$ is utilized in the calculation of the approximated cross section and the kinematical cut $\hat{s} > Q^2$ is imposed in the exact one.

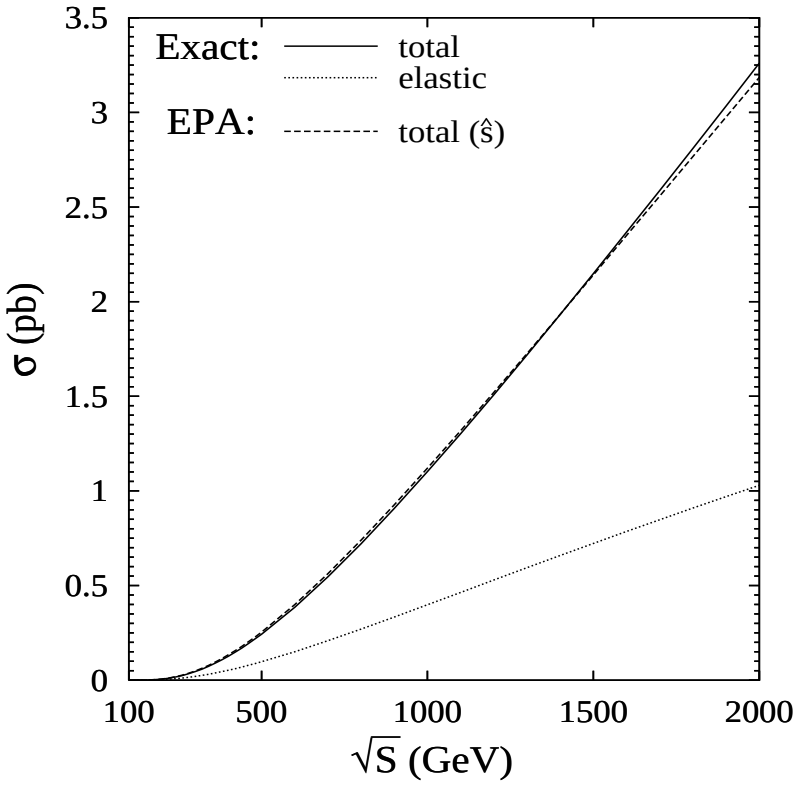

Fig. 4: Exact and approximated (EPA) total (= elastic + inelastic) cross sections of the process $ep \to \nu WX$ as functions of $\sqrt{S}$. The exact elastic component, which is indistinguishable from the approximated one, is shown separately.